Molecular Architecture of SMC proteins and the Yeast Cohesin Complex

Christian H. Haering[1,5], Jan Löwe[2,5], Andreas Hochwagen[1,3], and Kim Nasmyth[1,4]

[1]Research Institute of Molecular Pathology, Dr. Bohr Gasse 7, A-1030 Vienna, Austria; [2]MRC Laboratory of Molecular Biology Hills Road, Cambridge CB2 2QH, UK; [3]Present address: Center for Cancer Research, Massachusetts Institute of Technology, Cambridge, MA 02139, USA

[4]Correspondence: knasmyth@imp.univie.ac.at

[5]These authors contributed equally

SUMMARY

Sister chromatids are held together by the multi-subunit cohesin complex, which contains two SMC (Smc1, Smc3) and two non-SMC proteins (Scc1, Scc3). The crystal structure of a bacterial SMC "hinge" region along with EM studies and biochemical experiments on yeast Smc1 and Smc3 proteins show that SMC protamers fold up individually into rod-shaped molecules. A 45 nm long intra-molecular coiled coil separates the hinge region from the ATPase-containing "head" domain. Smc1 and Smc3 bind to each other via hetero-typic interactions between their hinges to form a V-shaped hetero-dimer. The two heads of the V-shaped dimer are connected by different ends of the cleavable Scc1 subunit. Cohesin therefore forms a large proteinaceous loop within which sister chromatids might be entrapped after DNA replication.

INTRODUCTION

When cells divide, not only must they duplicate all their chromosomes precisely but they must also segregate the two products, known as sister chromatids, to opposite poles of the cell prior to cytokinesis. Cohesion between sister chromatids has a crucial role during this process. It first enables cells to attach sister kinetochores to microtubules with opposing polarity (bi-orientation) and subsequently resists the tendency of these microtubules to pull chromatids towards opposite spindle poles (Nasmyth, 2001). An equilibrium between these two counteracting forces leads to the alignment of chromatid pairs on the metaphase plate. Finally, when all chromosomes have aligned on the spindle, the sudden destruction of cohesion triggers disjunction of chromatids and their traction towards opposite poles during anaphase.

Recent studies in the budding yeast *Saccharomyces cerevisiae* have identified five proteins that are essential for cohesion between sister chromatids: Scc1 (Mcd1), Scc3, Smc1, Smc3, and Pds5 (for review, see Nasmyth, 2001). Orthologs of all five proteins have been found in other eukaryotes so far studied and several have also been implicated in sister chromatid cohesion (Losada et al., 1998; Pasierbek et al., 2001; Sonoda et al., 2001). Scc1, Scc3, Smc1, and Smc3 are subunits of a soluble protein complex, called cohesin (Losada et al., 1998; Sumara et al., 2000; Toth et al., 1999). Pds5 also associates with cohesin but appears to be less tightly bound than the other four subunits.

In yeast, most cohesin remains associated with chromosomes until metaphase but dissociates at the onset of anaphase, when cohesion is dissolved. This event is triggered by cleavage of cohesin's Scc1 subunit by a cysteine protease, called separase (Uhlmann et al., 1999; Uhlmann et al., 2000). The bulk of cohesin in animal cells in contrast dissociates from chromatin during prophase/pro-metaphase in a separase independent manner. Nevertheless, a residual amount of cohesin remains associated with chromosomes, in particular around centromeres, until metaphase. This fraction behaves like the bulk of yeast cohesin, in that its cleavage is necessary for sister chromatid separation at the onset of anaphase (Hauf et al., 2001; Waizenegger et al., 2000). Cleavage of cohesin's Scc1 subunit may therefore be a universal trigger for chromosome segregation.

Cohesin's Smc1 and Smc3 subunits are both members of the SMC (<u>s</u>tructural <u>m</u>aintenance of <u>c</u>hromosomes) family of proteins, which exist in virtually all organisms including both bacteria and archaea (Soppa, 2001). SMC proteins share a 5-domain structure, with globular N- and C-terminal domains separated by a long (circa 100 nm or 900 residues) coiled coil segment in the centre of which is a globular "hinge" domain. All SMC proteins appear to form dimers, either forming homo-dimers with themselves, as in the case of prokaryotic SMC proteins, or hetero-dimers between different but related SMC proteins, as in the case of cohesin, which contains an Smc1/Smc3 hetero-dimer (see below) and condensin, which contains an Smc2/Smc4 hetero-dimer (Hirano et al., 1997).

An electron microscopic study of bacterial SMC proteins has established that their coiled coils are anti-parallel (Melby et al., 1998).

This orientation brings the N- and C-terminal globular domains (from either different or identical protamers) together, which unites an ATP binding site (Walker A motif) within the N-terminal domain with a Walker B motif (DA-box) within the C-terminal domain, to form a potentially functional ATPase of the ABC (ATP binding cassette) family (Hopfner et al., 2000; Löwe et al., 2001). The hinge domains of these bacterial SMC proteins are sufficiently flexible that the two head domains of a single homo-dimer can either be at opposite ends of a V-shaped molecule or in close juxtaposition of a stick-shaped one (Melby et al., 1998).

Despite these insights, it has never been established whether the two protamers of an SMC dimer contact each other along their entire length, as they would if the coiled coils were inter-molecular, or whether they do so merely in the hinge region, as they would if the coiled coils were intra-molecular. In the first case, the N- and C-terminal domains forming a head would be part of different molecules, whereas in the second, they would be the two ends of the same molecule (Fig. 2A). This issue has a crucial bearing on how Smc1 and Smc3 interact within the cohesin complex and its resolution is essential for understanding the geometry of not only of cohesin but also of condensin.

Much less is known about the structure of cohesin's other subunits. Scc1-like proteins are most conserved at their N- and C-termini. The two separase cleavage sites within yeast and mammalian Scc1 proteins are located in the centre of the protein between these two conserved domains. Importantly, cleavage at either site is sufficient to destroy cohesion at the metaphase to anaphase transition (Buonomo et al., 2000; Hauf et al., 2001; Uhlmann et al., 1999). Meanwhile, Pds5 (Neuwald and Hirano, 2000; Panizza et al., 2000) and Scc3 (D. Barford, personal communication) orthologs consist largely of HEAT repeats or HEAT repeat-like structures, respectively.

If we are to understand how cohesin links DNA molecules together, it is essential to know how cohesin's non-SMC subunits interact with Smc1 and Smc3. But to achieve this, it is crucial to establish first the fundamental geometry of the Smc1/3 hetero-dimer. By studying the architecture of Smc1 and Smc3 and by solving the structure of an SMC hinge domain associated with short coiled coils from the bacterium *Thermotoga maritima*, we have established that the coiled coils of many if not most SMC proteins are in fact intra-molecular. Cohesin therefore contains two long arms, one composed of Smc1 and the other of Smc3, which are connected at one end by hetero-typic interactions between their hinge domains. The other two ends, containing the ABC-like ATPase, can be connected by Scc1 whose N- and C-terminal domains bind to Smc3's and Smc1's heads respectively. This suggests a novel hypothesis for how cohesin associates with chromosomes and mediates cohesion between sisters.

We suggest that Scc1-mediated closure of cohesin's arms after a DNA strand has been embraced creates a topological link between these partners.

RESULTS

The SMC 'hinge domain' forms a doughnut-shaped dimer with all N- and C-termini located on one face.

Biochemical experiments involving the head domains of eukaryotic SMCs are only interpretable when it is known if their anti-parallel coiled coils segments are
intra- or inter-molecular, because this determines whether the heads are composed of N- and C-terminal domains from the same or different poly-peptide chains (Fig.2A). At issue here is the mechanism by which SMC proteins dimerize. In an attempt to address this, we solved the crystal structure of the SMC hinge domain from the bacterium *Thermotoga maritima*. A fragment containing residues 485-670 (HTMC2) crystallised in two different crystal forms, containing either one or two homo-dimers. The hinge domain crystal structures (Fig. 1) only reveal ordered residues from approx. 501 to 656. Residues 485 to 500 and 657 to 670 are invisible due to disorder, although they have been predicted to form a coiled coil. This is probably the case because the coiled coil segments are too short to be stable. It is however clear that the hinge domains are stable in the absence of ordered coiled coil segments. A DALI (Holm and Sander, 1995) search revealed no close structural homologues in the Protein Data Bank.

The hinge domain monomer is composed of two domains (I and II), which are related by a pseudo-twofold symmetry operation (Fig 1A). Domain I contains a short 3 stranded beta sheet flanked by two alpha helices whereas domain II contains a 5 stranded beta sheet also flanked by alpha helices. Inner helices (H4, H5, H9, H10) are involved in domain I/domain II interactions whereas outer ones (H6 and H11) are involved in dimer interactions. Domains I and II are linked by a long but ordered loop. An important feature of the monomer is that the fold separates the N- and C-termini of the same chain by 22 Å. The hinge domain dimer is formed by combining the beta sheets of two monomers into two 8 stranded beta sheets (Fig. 1B, C). This and the outer helices H6 and H11 are the only contacts holding the dimer together. It is worth noting that the first structure solved in spacegroup $P2_1$ contained a dimer in which one of the dimer contacts is disturbed by crystal contacts and the dimer has no true twofold axis. A second crystal form however contained dimers with true twofold symmetry (spacegroup $P2_12_12_1$) and we believe this is the biologically relevant conformation. The hinge dimer structure locates all N- and C-termini on one face of the doughnut-shaped structure. This explains EM pictures of SMC proteins where V-shaped or closed

conformations seem favoured (Anderson et al., 2002; Melby et al., 1998). The N- and C-termini from different monomers are closer together (13 Å) than the termini from the same monomer (22 Å). Nevertheless, both distances are compatible with the formation of coiled coils, leaving open whether the hinge seeds intra- or inter-molecular coiled coils. The crystal structure of a protein fragment containing longer coiled coil segments eventually settled this issue (see below). We meanwhile turned our attention to cohesin's Smc1 and Smc3 proteins, where the anticipated hetero-typic dimerization allowed us to address this issue in an independent manner.

Structure of Smc1/3 hetero-dimers and Smc3 monomers

To examine the structure formed by yeast cohesin SMC subunits, we first compared the hydrodynamic properties of Smc3 alone with that of complexes formed together with Smc1. We expressed Smc3 as an N-terminally His$_6$-tagged version either alone or together with Smc1 in insect cells. Both Smc3 and the Smc1/Smc3 complexes were found largely in the soluble cytosolic and nuclear fractions derived from the insect cell extracts. The proteins were partially purified over a nickel-affinity resin before determining Stokes radii and sedimentation coefficients by gel filtration and gradient centrifugation, respectively.

This yielded Stokes radii of 8.0 nm for the Smc1/His$_6$Smc3 complex and 7.4 nm for His$_6$Smc3 alone (Fig. 2B, top panels). Both the Smc1/His$_6$Smc3 complex and His$_6$Smc3 alone sedimented in sharp peaks in glycerol gradients; the former with a sedimentation velocity of 8.0S (which is similar to that of Xenopus Smc1/3 hetero-dimers) and the latter with 4.4S (Fig. 2B, lower panels).

The Stokes radii and sedimentation velocities were used to estimate native molecular weights using the method of Siegel and Monty (Siegel and Monty, 1966). This yielded a molecular weight of ~260 kDa for the Smc1/His$_6$Smc3 complex and ~130 kDa for His$_6$Smc3 alone, which are in good agreement with predicted molecular weights of 282 kDa for an (Smc1)$_1$/(Smc3)$_1$ hetero-dimer and 141 kDa for an Smc3 monomer. The large Stokes radii and low S-values, relative to globular proteins of similar molecular weight, are typical for elongated proteins. The equal intensities of the Smc1 and His$_6$Smc3 bands after silver staining (Fig. 2B) are also consistent with the Smc1/Smc3 complex being an equimolar hetero-dimer.

We next visualized the Smc1/3 hetero-dimer by electron microscopy after rotary shadowing. We obtained high resolution images that closely resembled those from prokarotic SMCs, which included the
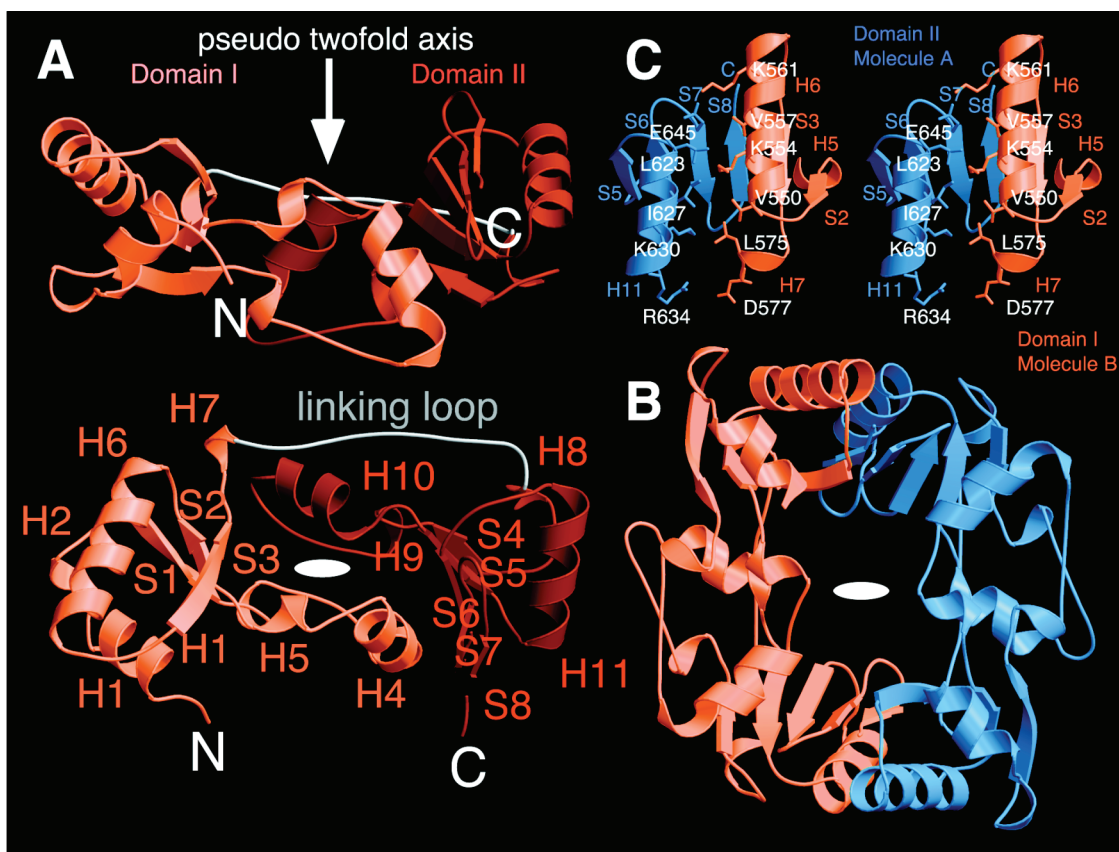
Figure 1 Crystal structure of the hinge domain from *Thermotoga maritima* SMC protein (construct HTMC2, residues 485-670). **(A)** Ribbon plot of one subunit of the hinge dimer solved in spacegroup P2$_1$ at 2.1 Å resolution by seleno-methionine substitution and MAD. Top and bottom view are rotated by 90° around the Y axis. **(B)** The hinge dimer is a doughnut-shaped structure. The structure shown has been solved in spacegroup P2$_1$2$_1$2$_1$ at 3.0 Å resolution (twinning fraction 0.158) by molecular replacement using the P2$_1$ high-resolution structure as starting model. **(C)** Stereo drawing of the dimer contact. The contact consists of an anti-parallel beta sheet contact of S3 and S8 and a helix/helix contact between H6 and H11. Residues highlighted are the only residues involved in the dimer contact. The corresponding residues in the yeast hinge domains of Smc1 and Smc3 would provide all specificity of hinge dimer formation. Figure prepared with MOLSCRIPT (Kraulis P.J., 1991).

different types of conformation seen for *E.coli* MukB and *B. subtilis* SMC proteins (Melby et al., 1998). The majority of molecules had an "open-V" or "Y" shaped conformation, in which the terminal head domains lie apart and the coiled coil arms are either separated over their whole or only part of their length, respectively (Fig. 2C). Some molecules showed kinks in their coiled coils, which might be an important feature to create the flexibility of the SMC arms. The Smc1/3 hetero-dimer also adopted the "coils spread" conformation, in which the head domains lie close together but the arms have bowed apart (Fig. 2C). With a total arm length of ~65 nm, consisting of a ~45 nm coiled coil stretch and head and hinge domains of about 10 nm diameter, the overall dimensions of the Smc1/3 hetero-dimer are similar to those of prokarotic SMCs. In contrast to a recent electron microscopy study on human and frog cohesin complexes (Anderson et al., 2002), yeast Smc1/3 hetero-dimers in the "open V" conformation had the arms separated at an average angle of only 35°, and angles of more than 60° were very rare. The similarity of the Stokes radii of Smc3 monomers and Smc1/3 hetero-dimers (Fig. 2B) also suggests that the two arms of the latter are rarely wide open.

These images, as well as those from prokaryotic SMCs, are consistent with both intra- and inter-molecular coiled coils (Fig. 2A). These two alternatives nevertheless make very different predictions as to the behavior and properties of single Smc1 or Smc3 protamers. If their coiled coils were intra-molecular, then individual SMCs should form stable rod shaped monomers containing a single coiled coil, with the hinge domain at one end and the globular head containing both N-and

C- terminal domains at the other. These monomeric rods would be equivalent to one arm of the hetero-dimer. If on the other hand they were inter-molecular, then the two amphipathic α-helices of a single SMC protamer would lack their dimerization partner. They might therefore no longer form a coiled coil and might instead adopt a disorganized structure with a propensity to aggregate.

The properties of Smc3 when expressed alone suggests that it forms intra-molecular coiled coils: Smc3 is soluble in the absence of Smc1 and sediments with a discrete 4.4S sedimentation velocity (Fig 2B). The same is true for Smc1 (data not shown). Under the electron microscope, we observed rod-like structures (65-70 nm in length) with a large globular domain at one end and a smaller one at the other (Fig. 2D). Most molecules had this configuration, which presumably corresponds to the "Smc3" arm of the hetero-dimer, with the larger globular domain containing Smc3's N- and C-terminal domains. To confirm this interpretation, we replaced Smc3's terminal domains by the 6-10 repeats from fibronectin, which can be identified as a short thick rod in electron micrographs (Melby et al., 1998). As expected, this resulted in replacement of the larger terminal globular domain by a pair of short rods with the dimensions expected for the fibronectin repeats (Fig. 2E).

SMC hetero-dimerization is conferred solely by hinge domains

While bacterial genomes usually encode only a single SMC-like protein, eukaryotic ones encode at least six different members (Soppa, 2001), which invariably act in pairs. Smc1 interacts with Smc3 in
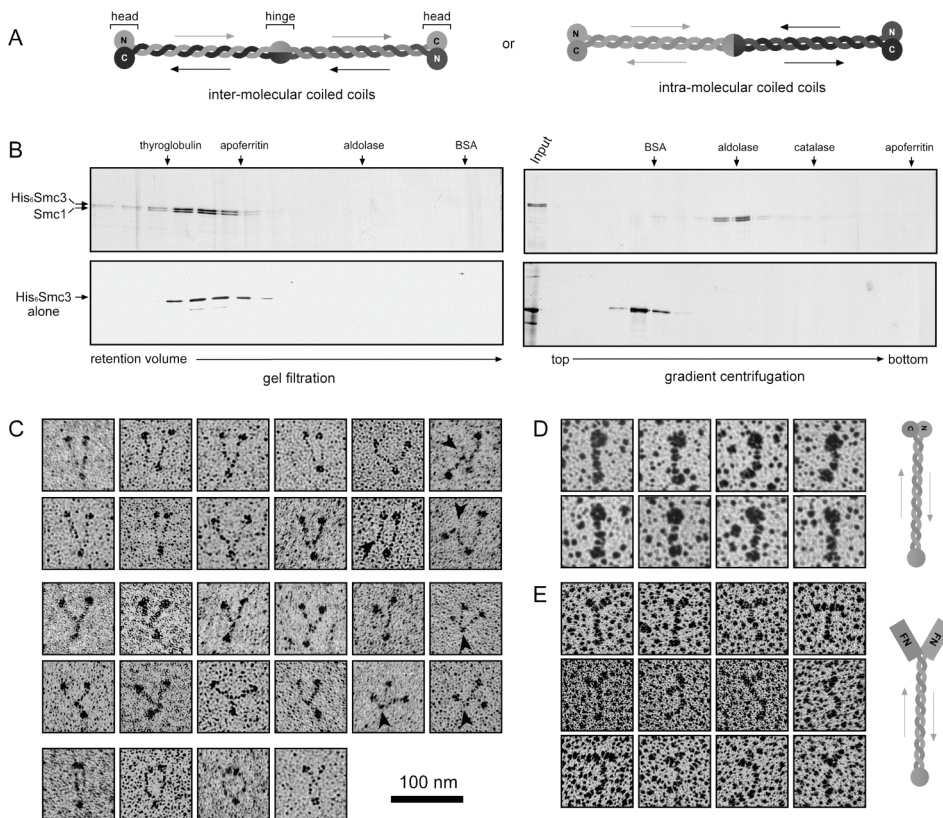
Figure 2 Smc1 and Smc3 form a V-shaped 1:1 hetero-dimer with intra-molecular coiled coils. **(A)** Two possible models of SMC dimerization. **(B)** Hydrodynamic properties of the Smc1/3 hetero-dimer and of the Smc3 monomer. Smc1 co-expressed with His$_6$Smc3 or His$_6$Smc3 expressed alone in insect cells were partially purified over Ni^{2+}-NTA. Imidazole eluates were run on a Sephacryl HR300 gel filtration column or on a glycerol gradient centrifugation. Proteins in gel filtration elution fractions (left panels) or in the fractionated gradient (right panels) were detected by silver staining after SDS-PAGE. **(C)** Electron micrographs of the Smc1/His$_6$Smc3 hetero-dimer. The Smc1/3 hetero-dimer from the gel filtration peak fraction was visualized in the electron microscope after rotary shadowing with a 1 nm platinum layer. Upper two rows: "open-V" conformation, middle two rows: "Y"-conformation, lower row: "coils spread" conformation. Arrows show kinks in the coiled coil arms (bar = 100 nm). **(D)** Electron micrographs of the Smc3 monomer. The His$_6$Smc3 monomer from the gel filtration peak fraction was visualized in the electron microscope after rotary shadowing with a 2 nm platinum layer. **(E)** Electron micrographs of chimeric fibronectin-Smc3 monomers. N- and C-terminal globular domains of His$_6$Smc3 were replaced by thick fibronectin segments and purified by Ni^{2+}- NTA and gel filtration. The purified monomers were rotary shadowed with a 1 nm platinum layer.

cohesin while Smc2 interacts with Smc4 in condensin. If SMC proteins form intra-molecular coiled coils, then the specificities of their pairwise interactions should be conferred solely by their hinge domains. A series of experiments in which we either removed or swapped hinge domains imply that possession of hetero-typic hinges is both necessary and sufficient for the interaction between Smc1 and
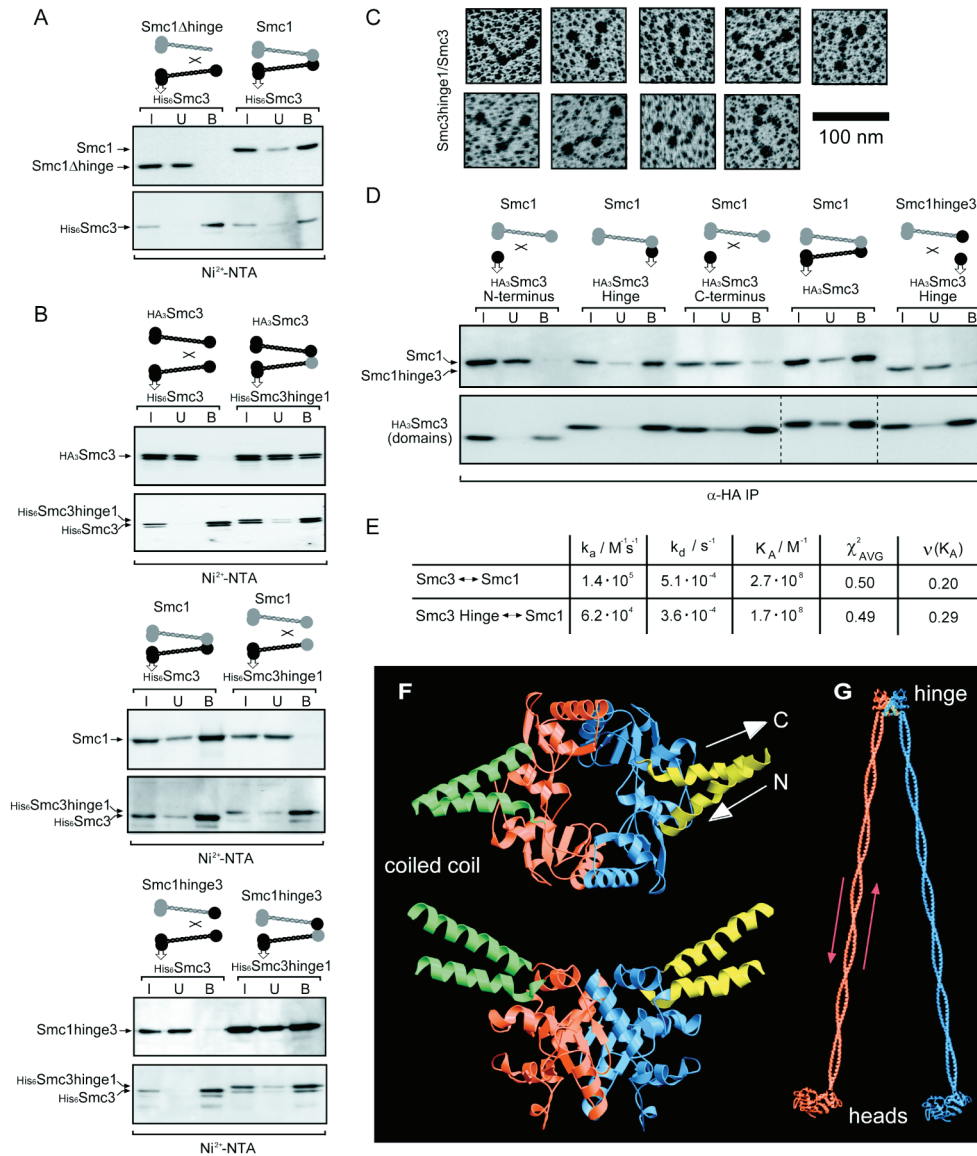
Figure 3. Smc1/3 dimerization specificity is solely conferred by the hinge domains. **(A)** The hinge domain is necessary for Smc1/3 dimerization. Smc1 hinge or Smc1 were co-expressed with His$_6$Smc3 in insect cells and subjected to a pull-down assay on Ni^{2+}-NTA. The presence of Smc1 hinge or Smc1 in input (I), unbound (U) and bound (B) fractions was probed by immunoblotting with an antibody specific to the N-terminus of Smc1 (upper panel) and the efficiency of Smc3 binding to the resin with anti-His antibody (lower panel). **(B)** Only molecules with opposite hinge domains can dimerize. Smc1, HA$_3$Smc3 or Smc1hinge3 were co-expressed in insect cells with either His$_6$Smc3 or His$_6$Smc3hinge1 and protein association of each combination was assayed as in (A). **(C)** Electron micrographs of the Smc3hinge1/Smc3 dimer. The His$_6$Smc3hinge1/ HA$_3$Smc3 dimer was purified from insect cells over Ni^{2+}-NTA and gel filtration. Proteins in the peak fraction from the gel filtration were rotary shadowed with a 2 nm platinum layer and visualized in the electron microscope. **(D)** The hinge domain of Smc3 is sufficient for binding to Smc1. N-terminal, hinge and C-terminal globular domains of Smc3 were co-expressed with Smc1 in insect cells as HA$_3$-tagged proteins. The globular domains were immunoprecipitated and their ability to pull down Smc1 was tested by immunoblotting for Smc1 (upper panel). Full-length HA$_3$Smc3 was used as a positive control. In addition, the association of the HA$_3$Smc3hinge domain with Smc1hinge3 was tested. In all experiments, the efficiency of the HA$_3$-immunoprecipitation was tested by blotting against the HA$_3$ epitope (lower panel). **(E)** The Smc3hinge domain binds Smc1 as tightly as the full-length Smc3 protein does. HA$_3$Smc3 or the HA$_3$Smc3hinge domain produced in insect cells were bound to a CM5 sensor chip on the BIAcore system via a monoclonal anti-HA antibody attached to covalently linked anti-mouse Fc γ specific antibody. Insect cell extracts containing defined concentrations of Smc1 as the ligand (five dilutions, ranging from 20 nM to 200 nM) were floated over the bound analytes, and association and dissociation kinetics were recorded. For each dilution, the data was fitted using a 1:1 Langmuir binding model with drifting baseline and corrected for unspecific binding to uninfected insect cell extracts. The average association and dissociation rate constants (k_a and k_d, respectively) are displayed and used to calculate the equilibrium binding constant (K_A). Low average values of χ^2 indicate the accuracy of the fit and the suitability of the 1:1 binding model, the variation coefficients ν for the binding constants show the consistency of the measurements over the ligand dilution range. **(F)** Crystal structure of the hinge domain from *Thermotoga maritima* SMC protein (construct HTMC9, residues 473-685). Ribbon drawing of the hinge domain dimer, showing two stretches of anti-parallel coiled coil (yellow and green). The orientation is essentially the same as in figure 1B. The coiled coil segments are formed by residues from the same chain, resulting in an intra-molecular coiled coil arrangement for SMC proteins. The structure shown was re-solved in spacegroup C2 by seleno-methionine substitution and MAD at 3.0 Å resolution. **(G)** Architecture of SMC proteins. The intra-molecular coiled coil results in the two arms being formed by separate chains with the hinge domains holding the two arms together. The coiled coil segments have been modelled using standard geometry and the crystal structures of the hinge and head domains have been described here and elsewhere (Löwe et al., 2001). Figure prepared using MOLSCRIPT (Kraulis P.J., 1991).

Smc3. A version of Smc1 whose hinge domain was replaced by a short peptide linker (Smc1 hinge) failed to bind Smc3 (Fig. 3A). While Smc3 cannot bind to a differently tagged version of the same protein (Fig. 3B, top panel), a chimeric version of Smc3 whose hinge (and hinge alone) had been replaced by that of Smc1 (Smc3hinge1) bound to Smc3 (Fig. 3B top, panel) but not to Smc1 (Fig. 3B, middle panel). Finally, a chimeric version of Smc1 with an Smc3 hinge did not bind to Smc3 itself but bound to Smc3 containing Smc1's hinge (Fig. 3B, bottom panel). Remarkably, the complex formed between Smc3 and the chimeric Smc3hinge1, which only contains coiled coil sequences from Smc3, eluted from a gel filtration column at an identical position to that of Smc1/3 dimers (not shown) and adopted a similar set of structures when viewed by electron microscopy, including the "open" V-shaped conformation (Fig. 3C). This last result is easy to explain if the Smc1/3 hetero-dimer's coiled coils were intra-molecular but difficult if they were inter-molecular.

Even when expressed alone, Smc3's hinge domain but neither its N- nor C-terminal domains bound to Smc1 with an efficiency similar to that of intact Smc3 (Fig. 3D). In contrast, Smc3's hinge domain failed to bind the chimeric Smc1 molecule with a hinge derived from Smc3. If interaction between hetero-typic hinges were the sole means by which Smc1 and Smc3 were held together, then the affinity of an isolated Smc3 hinge for Smc1 might be expected to be similar to that of intact Smc3 protein. To investigate this, we used BIAcore solid state affinity measurements to estimate on-rate (k_a), off-rate (k_d) and affinity ($K_A=k_a/k_d$) constants by measuring the on- and off-rates of Smc1 binding to immobilized intact Smc3 or Smc3 hinge alone at different concentrations (Fig. 3E). The off-rates of Smc3 and its hinge alone were very similar and correspond to a half life of ~25 min, whereas the on-rate of Smc3 was about twice that of its hinge. This difference could easily be due to steric factors; namely, the hinge may be more accessible to Smc1 when situated at the end of a long coil than when more closely bound to the BIAcore matrix. The calculated affinity constants for both types of molecules are around ~$2 \cdot 10^8/M^{-1}$, indicative of a very strong interaction. These data imply that Smc3's coiled coil region makes little or no contribution to its Smc1 binding
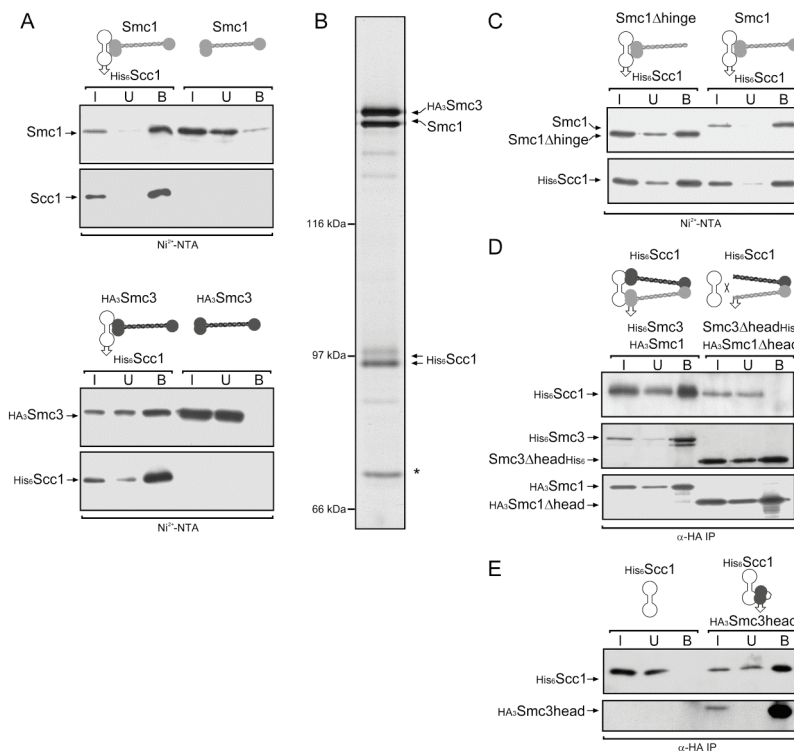
Figure 4 Smc1 and Smc3 bind to Scc1 via their head domains. **(A)** Smc1 and Smc3 individually bind to Scc1. Smc1 and HA$_3$Smc3 were expressed separately or co-expressed with His$_6$Scc1 in insect cells. Protein extracts were subjected to a pull-down assay on Ni^{2+}-NTA. The presence of Smc1 or Smc3 in input (I), unbound (U) and imidazol-eluate (bound, B) fractions was probed with anti-Smc1 or anti-HA specific antibodies on immunoblots, the efficient binding of His$_6$Scc1 to the resin is shown by probing with anti-His antibody. **(B)** Scc1 binds stably to the Smc1/3 hetero-dimer. His$_6$Scc1, Smc1 and HA$_3$Smc3 were co-expressed in insect cells and purified over Ni^{2+}-NTA and gel filtration. No major bands besides the three cohesin subunits were detected in a silver stain of the peak elution fraction, except one band (*) which was identified to consist of Hsp70 chaparone family protein by mass-spectrometry. A minor portion of Scc1 is phosphorylated (upper band of His$_6$Scc1). **(C)** The Smc1 hinge domain is not necessary for Smc1 association with Scc1. Smc1 hinge or Smc1 were co-expressed with His$_6$Scc1 and used in binding experiments to Ni^{2+}-NTA as in (A). **(D)** The Smc1/3 head domains are necessary for Scc1 binding. HA$_3$Smc1 and His$_6$Smc3 or HA$_3$Smc1 head and Smc1 head His$_6$ were co-expressed with His$_6$Scc1. The wild type or head-less Smc1/3 hetero-dimers were pulled down by anti-HA immunoprecipitation and co-precipitation of His$_6$Scc1 was probed on an anti-His immunoblot (upper panel). Effective immunoprecipitation of the Smc1/3 hetero-dimer is shown by probing for His$_6$Smc3(head) and HA$_3$Smc1(head) (middle and lower panel). **(E)** The Smc3head domain is sufficient for Scc1 binding. N- and C-terminal globular domains of Smc3 were fused by a short linker to generate an isolated Smc3 head domain. His$_6$Scc1 was expressed with and without HA$_3$Smc3head domain in insect cells and subjected to anti-HA immunoprecipitation.

affinity, which is consistent with the coiled coils being intra- and not inter-molecular.

SMC molecules form intra-molecular coiled coils

To re-examine whether the bacterial SMC also form intra-molecular coiled coils, we attempted crystallisation of *T. maritima* SMC hinge domain fragments containing longer adjacent coiled coil sequences. Only one such construct (aa 473-685, HTMC9) produced crystals. To obtain an unbiased view, the structure was re-solved with independent phases using seleno-methionine substituted protein and MAD at 3.0 Å resolution in spacegroup C2 (Fig. 3F). Again, the crystals contain exclusively dimers. The core dimer of the hinge domain is essentially the same as described in Fig. 1. However, this time coiled coil segments are clearly visible. The helices are as expected anti-parallel but they originate from the same chain, which implies that *T. maritima*'s SMC contains intra-molecular coiled coils. A properly scaled model of SMC proteins resulting from the above studies and earlier structural work on the head domains (Löwe et al., 2001) is shown in Fig. 3G. Several conclusions follow from this general architecture. The hinge dimer is the only part of the structure holding the more than 100 nm long SMC dimer together. Only a few residues

in the hinge dimer interface (Fig. 1C) contribute to this interaction. Secondly, the intra-molecular coiled coil ensures that the head domains are composed of N- and C-terminal domains from a single SMC chain, as predicted by our biochemical experiments with yeast Smc1 and Smc3. Our structure is therefore consistent with the notion that one of cohesin's heads is composed of N- and C-terminal domains from Smc1 while the other is composed of N- and C-terminal domains from Smc3.

Scc1 binds to the head domains of Smc1 and Smc3

Having established the geometry of Smc1/3 hetero-dimers, we next investigated how they interact with cohesin's other subunits. We first tested whether Scc1 binds to the Smc1/3 hetero-dimer. Both the hetero-dimer and individual Smc1 and Smc3 monomers bound efficiently to Scc1 when co-expressed in insect cells (Fig. 4A and D). The hetero-dimer furthermore co-purified in a complex with Scc1 in a gel filtration column (Fig. 4B). The only major contaminant was a Hsp70 chaperone protein, which was found to be associated with baculovirus expressed Scc1 previously (Uhlmann et al., 2000). Replacement of Smc1's hinge domain with a short peptide linker had little or no effect on its ability to bind Scc1 (Fig. 4C). In contrast,
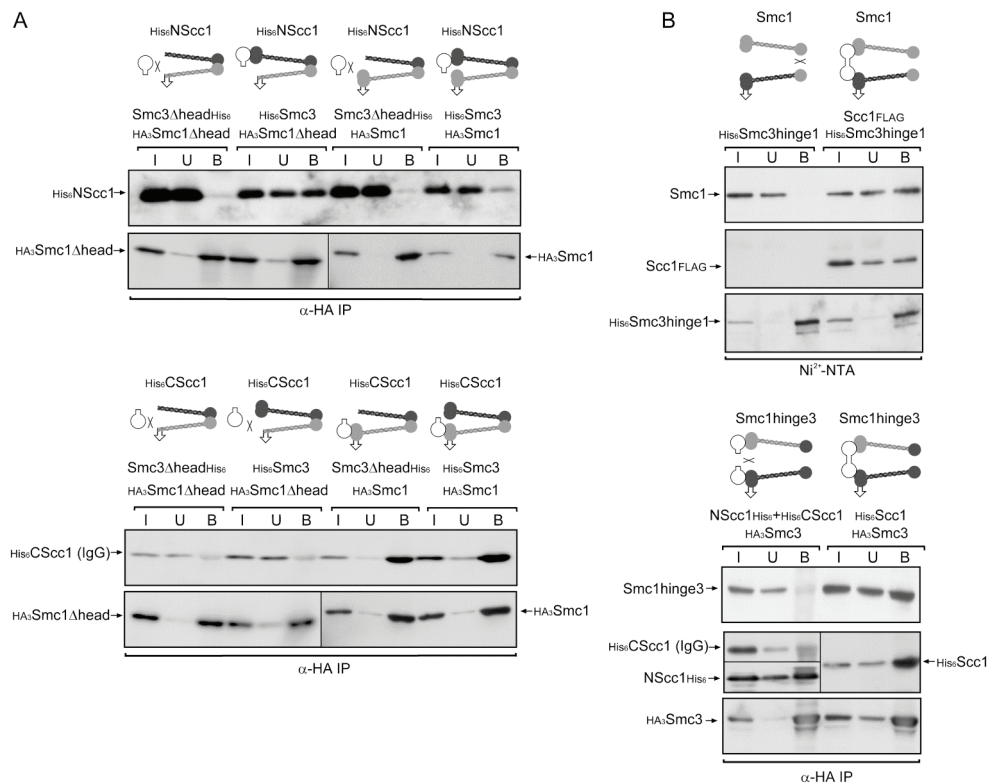
Figure 5 Scc1 links the head domains of Smc1 and Smc3. (A) The Smc1 head domain binds to the C-terminal Scc1 separase cleavage fragment, the Smc3 head domain to the N-terminal fragment. Smc1/3 hetero-dimers lacking both head domains, lacking only the Smc1 or Smc3 head domain or wild type hetero-dimers were co-expressed with either the N-terminal or C-terminal separase cleavage fragment of Scc1 in insect cells. The hetero-dimer combinations were immunoprecipitated by the HA$_3$-epitope tag on Smc1 or Smc1 head, respectively, and co-precipitation of the His$_6$-tagged Scc1 fragments was probed by immunoblotting against the His$_6$ epitope (upper panels). The C-terminal separase cleavage fragment co-migrates with the IgG heavy chain, resulting in background signals in the bound (B) fractions. The efficiency of the immunoprecipitation is shown by probing the immunoblots with anti-HA specific antibody (lower panels). (B) Intact Scc1 can bring together Smc1 and Smc3 which have lost the ability to dimerize via their hinges. Smc1 and His$_6$Smc3hinge1 were co-expressed by themselves or together with Scc1 in insect cells (top). Protein extracts were run over a Ni^{2+}-NTA resin and eluted with imidazole. Presence of Smc1 in the fractions was followed by immunoblotting with anti-Smc1 specific antibody. Binding of His$_6$Smc3hinge1 and Scc1 to the resin was confirmed by probing with specific antibody to the FLAG epitope tag on Scc1 and to the His$_6$ epitope. Smc1hinge3 and HA$_3$Smc3 were co-expressed with both, N-and C-terminal Scc1 cleavage fragments or full length Scc1 (bottom). HA$_3$Smc3 was immunoprecipitated. Co-immunoprecipitation of Smc1hinge3 was tested by probing with Smc1-specific antibody. Full length Scc1 and both Scc1 fragments were His$_6$-tagged, allowing detection with anti-His$_6$ specific antibody. Effective immunoprecipitation of HA$_3$Smc3 was confirmed by probing with anti-HA antibody.

removal of both head domains from the Smc1/3 hetero-dimer abolished its ability to bind Scc1, even though the head-less SMCs bound to each other efficiently to form a soluble complex (Fig. 4D). To test whether Smc3's head alone is sufficient to bind Scc1, we created an artificial head in which Smc3's N-terminal domain was connected to its C-terminal domain by a short peptide linker. This isolated Smc3 head bound Scc1 efficiently (Fig. 4E). Addition of short stretches of the coiled coil normally attached to this head did not augment Scc1's association with Smc3's head (data not shown).

N- and C-terminal Scc1 cleavage fragments bind to Smc3 and Smc1 heads respectively

Scc1's cleavage by separase is necessary and sufficient to destroy sister chromatid cohesion. To shed light on the molecular mechanism of this crucial step, we next investigated the ability of Scc1's N- and C-terminal cleavage fragments to bind Smc1 and Smc3. To do this, we created recombinant baculoviruses that express either an N-terminal Scc1 fragment, from the N-terminus to the first separase cleavage site (aa 1-180), or a C-terminal Scc1 fragment, from the second separase cleavage site to the C-terminus (aa 269-566), tagged with six histidine-residues. Remarkably, both bound to the Smc1/3 hetero-dimer when co-expressed with Smc1 and Smc3 (data not shown). When Smc1 or Smc3 separately were co-expressed with the

Scc1 fragments, Smc1 bound weakly to the N-terminal but strongly to the C-terminal cleavage fragment, while Smc3 only bound to the N-terminal but not to the C-terminal fragment (see Supplemental Fig. S1 at http://www.cell.com/molecular-cell/supplemental/S1097-2765(02)00515-4). Co-immunoprecipitation of Smc1 with Scc1's C-terminal cleavage fragment has also been detected in yeast extracts (Rao et al., 2001).

Together with the finding that intact Scc1 binds to the hetero-dimer's head domains, these data suggest that Scc1's N- and C-terminal fragments bind to Smc3's and Smc1's head domains respectively. To test this, we co-expressed each Scc1 fragment with hetero-dimers lacking both heads, lacking only that of Smc1, or lacking only that of Smc3. As predicted, Smc1/3 dimers lacking both heads bound neither N- nor C-terminal Scc1 fragment, Smc1/3 dimers missing only Smc1's head bound Scc1's N-terminal but not it's C-terminal fragment, whereas Smc1/3 dimers missing only Smc3's head bound Scc1's C-terminal but not N-terminal fragment (Fig. 5A). The weak binding of Scc1's N-terminal fragment to Smc1 (Supplemental Fig. S1) is presumably due to an interaction with its exposed hinge domain, because this association is abolished when Smc1's hinge is attached to a head-less Smc3 (Fig. 5A) or an isolated Smc3 hinge domain (Supplemental Fig. S1), or when Smc1's hinge is replaced by that of Smc3 (data not shown). In all cases, the binding to the C-
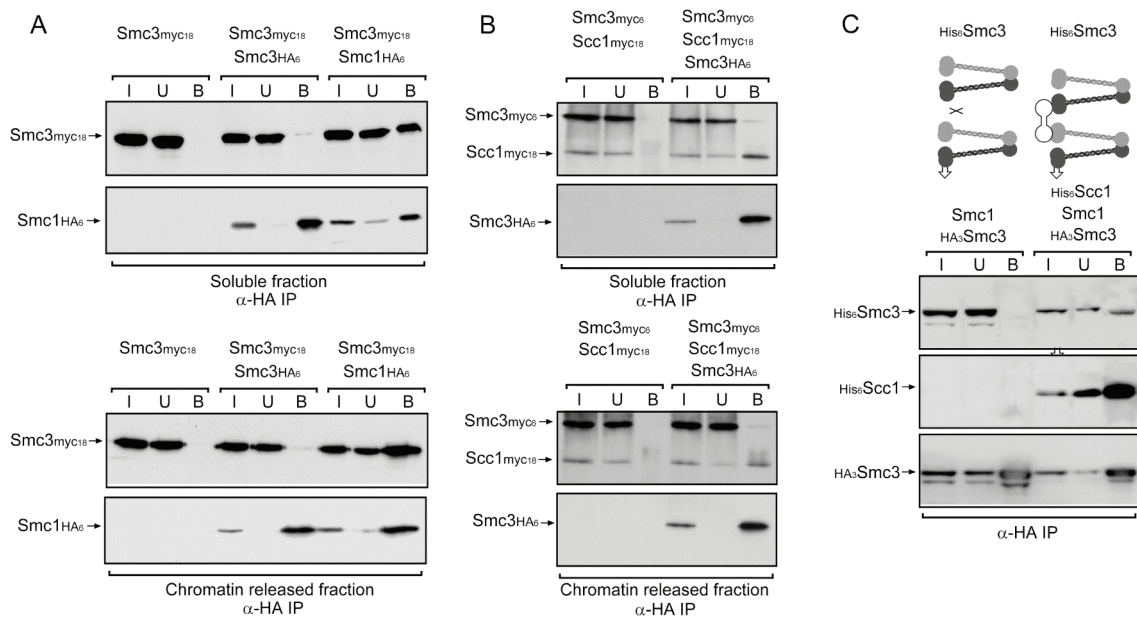
Figure 6 Only one copy of Smc1 and Smc3 proteins present in cohesin complexes isolated from yeast. **(A)** Only one Smc3 in a single cohesin complex. Extracts were prepared from yeast strains expressing the indicated epitope-tagged versions of Smc1 or Smc3 (K6396, K10036, K10037). Soluble extracts were separated from chromatin, and cohesin complexes were released from chromatin by micrococcal nuclease digestion. Soluble and chromatin-released extract fractions were used in immunoprecipitation experiments against the HA_6 epitope tag, and co-immunoprecipitation of myc_{18} tagged proteins was probed with anti-myc specific antibodies in immunoblots (upper panels). Efficient immunoprecipitation of HA-tagged Smc1 and Smc3 proteins was confirmed by probing with anti-HA antibodies (lower panels). **(B)** Scc1 is associated with immunoprecipitated Smc3. As in (A), using strains expressing the indicated tagged Smc3 and Scc1 versions (K10039, K10038). **(C)** Scc1 is capable of binding two different Smc1/3 hetero-dimers when overexpressed in insect cells. Smc1 together with His_6- and HA_3- tagged versions of Smc3 were co-expressed in insect cells with and without His_6Scc1. After immunoprecipitation of Smc1/3 hetero-dimers containing HA_3Smc3, co-precipitation of His_6Smc3 containing hetero-dimers was probed by immunoblotting with His_6- specific antibody (upper panel). HA_3Smc3 and His_6Scc1 were efficiently immunoprecipitated (middle and lower panel).

terminal fragment is maintained.

Though these results demonstrate that Scc1 possesses two different binding sites for separate heads of the Smc1/3 hetero-dimer, they do not address whether a single Scc1 molecule can bind to Smc1 and Smc3 heads simultaneously. If this occurs, then monomeric Scc1 should be able to link Smc1 and Smc3 together independently of any interaction between their hinges. We therefore investigated whether Scc1 can join Smc1 with the Smc3 chimera containing Smc1's hinge (Smc3hinge1). These two SMC proteins possess Smc1 and Smc3 head domains respectively but cannot bind to each other because they have homo-typic hinges. They nevertheless co-purified when co-expressed with intact Scc1 (Fig.5B top). Likewise, Smc3 can be co-precipitated with Smc1 containing Smc3's hinge if these two proteins are co-expressed with intact Scc1, but not when co-expressed with Scc1's N- and C-terminal cleavage fragments (Fig. 5B bottom). Because other experiments (see below) suggest that Scc1 cannot link Smc1 and Smc3 heads by virtue of its own multimerization, we conclude that a single Scc1 molecule can bind simultaneously to the head domains of Smc1 and Smc3 and thereby form a bridge between them.

Most cohesin complexes in yeast contain only a single Smc1/3 hetero-dimer

The presence of two independent SMC interaction sites within Scc1, one binding to Smc1's head and the other to that of Smc3, gives rise to two possibilities. Scc1 could link Smc1 and Smc3 heads either from the same hetero-dimer or from two different ones. To add on this issue, we created a diploid yeast strain in which one Smc3 gene was tagged with the myc18 epitope and the other with the HA6 epitope. Micrococcal nuclease digestion was used to release cohesin from chromatin (Ciosk et al., 2000), which had previously been separated from a "soluble" cell fraction (Liang and Stillman, 1997; Uhlmann et al., 1999). We immunoprecipitated Smc3HA6 from both "soluble" and "chromatin released" fractions and used Western blotting to measure co-precipitation of Smc3myc18 (Fig. 6A). Little or no Smc3myc18 was detectable in Smc3HA6 immunoprecipates from either fraction. It was nevertheless efficiently co-immunoprecipitated with Smc1HA6 from extracts prepared from a diploid in which Smc1 (and not Smc3) was tagged with the HA6 epitope. When we used diploid strains expressing myc18-tagged Smc1 plus either Smc1HA6 or Smc3HA6, little or no Smc1myc18 co-immunoprecipitated with Smc1HA6, but Smc1myc18 was efficiently co-immunoprecipitated with Smc3HA6 (data not shown). To exclude the possibility that cohesin complexes fall apart during the preparation of these extracts, we repeated the experiment using a diploid strain expressing myc6 and HA6 tagged Smc3 proteins and a myc18 tagged Scc1 protein. Scc1myc18 but little or no Smc3myc6 co-precipitated with Smc3HA6 (Fig. 6B). Thus, Smc3 molecules co-precipitate with those of Smc1 and Scc1 (from both soluble and chromatin-released fractions) but rarely if ever with other molecules of Smc3. This suggests that few if any different Smc1/3 hetero-dimers are linked together by Scc1 in yeast, which is contrary to the proposal
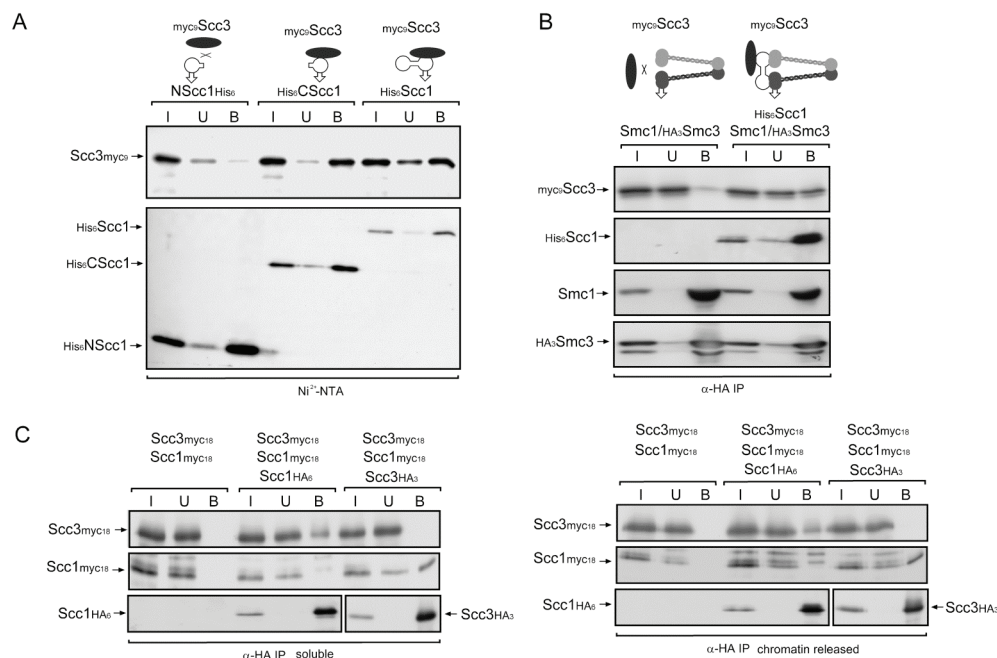
Figure 7 Model of the yeast cohesin complex. **(A)** Smc1 and Smc3 form a hetero-dimer with intra-molecular coiled coils. Scc1 bridges the head domains of Smc1 and Smc3 and links them to Scc3. For comparison, a schematic 10 nm chromatin fibre of DNA wrapped around nucleosomes and a DNA double helix are shown in scale to the Smc1/3 ring. **(B)** Hypothetical 'embrace' model how the cohesin complex might confer sister chromatid cohesion. Before the commencement of replication, the cohesin complex is loaded onto DNA. The arms of the Smc1/3 molecules embrace the DNA, thereby forming a ring of approx. 40 nm diameter. The head domains of Smc1 and Smc3 are locked together by Scc1. Now, cohesion might be generated as the replication fork passes through the ring, entrapping both sister chromatids inside. At the metaphase to anaphase transition, Scc1 is cleaved by separase, thereby opening the lock of the Smc1/3 head domains. The ring opens and sister chromatids can be pulled to opposite spindle poles.

that Scc1 links two hetero-dimers each bound to a sister chromatid (Uhlmann et al., 1999). The corollary is that individual Scc1 molecules normally bind to the Smc1 and Smc3 heads of a single hetero-dimer. Scc1 is nevertheless capable of linking differently marked Smc1/3 hetero-dimers when these proteins are over-produced from baculoviruses in insect cells (Fig. 6C), possibly because of unnaturally high protein concentrations.

Scc1 links Scc3 to the Smc1/3 hetero-dimer

To investigate how cohesin's fourth subunit, Scc3, binds to the other three constituents, we first expressed a myc_9 epitope tagged Scc3 protein (myc_9Scc3) in insect cells along with either full length His_6 tagged Scc1 or its N- or C-terminal separase cleavage fragments. The amount of Scc3 associated with each Scc1 protein purified on Ni^{2+}-NTA was measured by Western blotting (Fig. 7A). Scc3 co-purified with full length Scc1 and its C-terminal fragment but not with its N-terminal fragment. This suggests that Scc3 binds Scc1 via Scc1's C-terminus. To determine whether Scc3 also binds directly to the Smc1/3 hetero-dimer, we co-expressed myc_9Scc3 together with an Smc1/3 hetero-dimer whose Smc3 protein was tagged with HA epitopes. Little or no myc_9Scc3 co-precipitated with the Smc1/3 hetero-dimer when immunoprecipitated via Smc3's HA_3 tag, but much more did so when Scc1 was expressed in the same cells (Fig. 7B). A similar result was obtained when the experiment was performed using Smc1-specific antibodies to immunoprecipitate the Smc1/3 dimer (data not shown). These data suggest that Scc3 does not directly bind the Smc1/3 hetero-dimer but is linked to it by Scc1.

Cohesin contains only a single molecule of Scc1 and Scc3

To address whether the cohesin complex contains one or more Scc3 subunits, we co-expressed myc_9 tagged Scc3 along with a Scc3 version tagged with ten histidine residues (His_{10}) in insect cells. $His_{10}Scc3$ and myc_9Scc3 neither co-purified when Scc3 was immunoprecipitated using myc-specific antibodies nor when $His_{10}Scc3$ was bound to Ni^{2+}-NTA (data not shown). Co-purification was undetectable even when $His_{10}Scc3$ and myc_9Scc3 were co-expressed along with Scc1, Smc1 and Smc3. Likewise, a His_6 tagged version of Scc1 failed to co-purify with a FLAG tagged version of Scc1 fused to a chitin binding domain (data not shown). Thus, neither Scc1 nor Scc3 bind to themselves when over-expressed in insect cells. These data suggest that cohesin contains only a single molecule of Scc3. To verify this, we created a diploid yeast strain that expressed $Scc1myc_{18,}$ $Scc3myc_{18}$ from one allele and $Scc3HA_3$ from the other. $Scc1myc_{18}$ but not $Scc3myc_{18}$ co-precipitated with $Scc3HA_3$ from soluble and chromatin-released extracts (Fig. 7C). This confirms that there is only a single Scc3 molecule in each yeast cohesin complex. It

also implies that the same must be true for Scc1, because it binds directly to Scc3. To test this directly, we repeated the above experiment using a yeast strain expressing $Scc1myc_{18}$ and $Scc1HA_6$ as well as $Scc3myc_{18}$. As expected, $Scc3myc_{18}$ but not $Scc1myc_{18}$ co-immunoprecipitated with $Scc1HA_6$ (Fig. 7C). The fact that all tagged proteins are functional in vivo (Toth et al., 1999) and that $Scc1myc_{18}$ and $Scc3myc_{18}$ co-precipitate with $Scc3HA_6$ and $Scc1HA_6$ respectively implies that all these epitope tagged proteins are indeed assembled into cohesin complexes. Our data suggest that cohesin contains only a single molecule each of Scc1 and Scc3.

DISCUSSION

Both eukaryotic and prokaryotic SMC proteins form intra-molecular coiled coils

Studies of bacterial SMC proteins (Löwe et al., 2001; Melby et al., 1998) have hitherto failed to determine whether their arms are composed of inter- or intra-molecular coiled coils. Because eukaryotic SMCs are thought to form hetero-dimers, the arrangement of their coiled-coils has a crucial bearing on the composition of their heads; that is, whether they are composed of N- and C-termini from the same or different SMC protein. Reasoning that all SMCs would use the same arrangement and that the structure of any one hinge domain might reveal the exit path of their coiled coils, we determined the crystal structure of the hinge domain of SMC from the bacterium *T. maritima*. The structure showed that isolated hinges form donut-shaped dimers and that both N- and C-termini emerge from the same face, which explains why the coiled coil arms of SMC proteins form open or closed V shapes, but did not reveal whether the termini seed intra- or inter-molecular coiled coil formation.

Though no ordered coiled coils were visible in our first *T. maritima* hinge structure, biochemical analysis of Smc1 and Smc3 strongly suggests that these SMC proteins form intra-molecular coiled coils. Smc1 and Smc3 exist as monomers when expressed alone in insect cells, but when co-expressed exist as 1:1 hetero-dimers, whose appearance under the electron microscope resembles that of *B. subtilis* SMC homo-dimers. Electron microscopy of Smc3 molecules on their own showed that they exist as rods with a small globular domain at one end and a larger one at the other. The latter must be jointly composed of its N- and C-terminal domains because their replacement by fibronectin repeats gives rise to a pair of short thick rods instead. Remarkably, replacement of Smc3's hinge domain by that of Smc1 results in an Smc3 chimera which forms a hetero-dimer with wild-type Smc3 resembling that normally formed between Smc1 and Smc3. These data suggest that the Smc1/3 hetero-dimer is formed by hetero-typic interactions solely between the hinges of Smc1 and Smc3 and that each arm is composed of coiled coils created by folding back each

molecule on itself, with its hinge as the folding axis. As predicted by this model, an isolated hinge from Smc3 binds to Smc1 almost as tightly as the intact molecule.

With these insights, we revisited the geometry of *T.maritima*'s hinge and solved the crystal structure of a longer hinge segment, whose ordered coiled coils clearly revealed them to be intra-molecular. Because SMC proteins are presumably descended from an ancestral bacterial protein, we suggest that all proteins of this family form intra-molecular coils and are joined together by homo- (prokaryotes) or hetero- (eukaryotes) typic interactions solely between their hinge domains. The finding that mutation of conserved glycine residues within the hinge domain of *B.subtilis* SMC proteins causes them to accumulate as monomers resembling those of Smc1 or Smc3 when expressed without the other (Hirano et al., 2001) is consistent with this notion. These glycines are situated in the dimer interaction surface and their mutation would be expected to disrupt hinge dimerization. Intra-molecular coiled coils may also be the rule for more distant relatives of the SMC family such as Rad50 (de Jager et al., 2001), which lack globular hinge domains to form stable dimers. Formation of intra-molecular coiled coils is furthermore far easier to envisage in terms of protein folding than the inter-molecular ones initially proposed for SMC proteins.

Scc1 binds to the heads of Smc1 and Smc3

Our discovery that the Smc1/3 hetero-dimer has in all likelihood one arm composed of Smc1 and another of Smc3 turned out to be crucial in understanding how it interacts with cohesin's other subunits. Of these, only its cleavable Scc1 subunit binds directly to the Smc1/3 hetero-dimer. Scc1 also binds directly to Scc3 and thereby links this subunit to the Smc1/3 hetero-dimer. It is presumably no coincidence that it is cleavage of this central subunit which triggers loss of sister chromatid cohesion at the metaphase to anaphase transition (Hauf et al., 2001; Uhlmann et al., 1999).

Several lines of evidence suggest that Scc1's N-terminal half binds to Smc3's head whereas its C-terminal half binds to that of Smc1. Intact Scc1 binds to Smc1/3 hetero-dimers lacking either Smc1's head or that of Smc3 but not both, whereas its N-terminal fragment binds to hetero-dimers lacking Smc1's but not Smc3's head, and Scc1's C-terminal fragment binds to hetero-dimers lacking Smc3's but not Smc1's head. Scc1 cannot itself dimerize, but because it has two separate binding sites for Smc1 and Smc3, it is capable linking the heads of these two proteins together even when they are prevented from interacting via their hinges. These observations raise the possibility that the two arms of the Smc1/3 hetero-dimer are linked not only through interaction between their hinges but also by the binding of their heads to different ends of a single Scc1 molecule. When and if this occurs, cohesin would form a closed proteinaceous
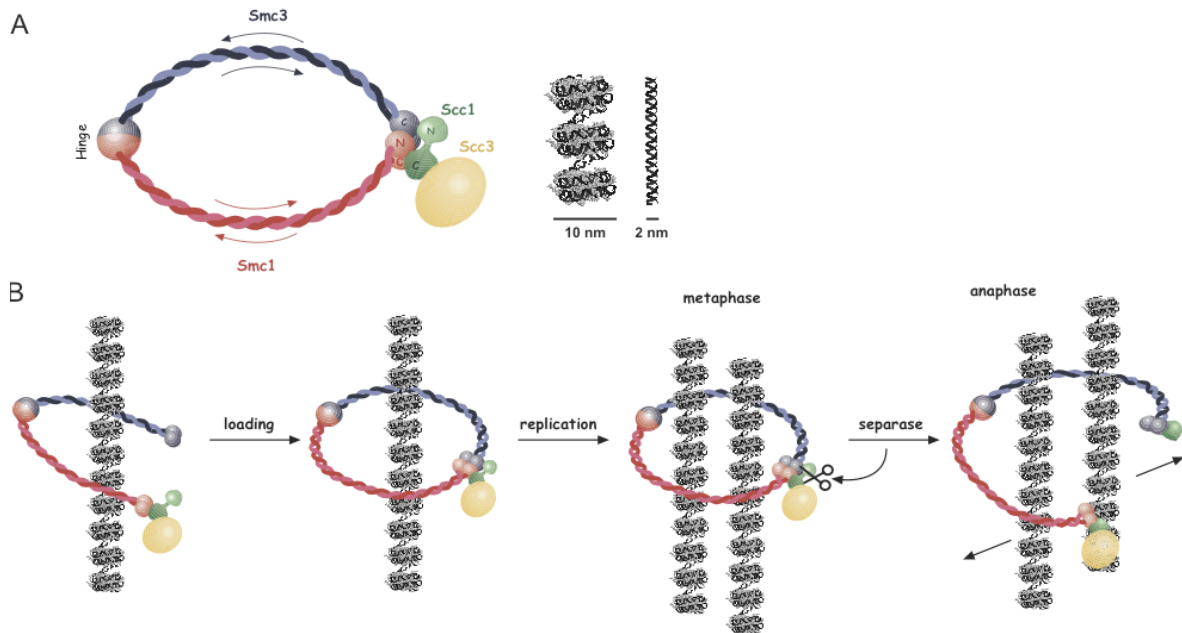
Figure 8 Model of the yeast cohesin complex. **(A)** Smc1 and Smc3 form a hetero-dimer with intra-molecular coiled coils. Scc1 bridges the head domains of Smc1 and Smc3 and links them to Scc3. For comparison, a schematic 10 nm chromatin fibre of DNA wrapped around nucleosomes and a DNA double helix are shown in scale to the Smc1/3 ring. **(B)** Hypothetical 'embrace' model how the cohesin complex might confer sister chromatid cohesion. Before the commencement of replication, the cohesin complex is loaded onto DNA. The arms of the Smc1/3 molecules embrace the DNA, thereby forming a ring of approx. 40 nm diameter. The head domains of Smc1 and Smc3 are locked together by Scc1. Now, cohesion might be generated as the replication fork passes through the ring, entrapping both sister chromatids inside. At the metaphase to anaphase transition, Scc1 is cleaved by separase, thereby opening the lock of the Smc1/3 head domains. The ring opens and sister chromatids can be pulled to opposite spindle poles.

loop (Fig. 8A). Whether cohesin actually forms such loops when it binds to chromosomes and participates in sister chromatid cohesion is clearly an important question for future experiments. The recent finding that non-SMC material associated with soluble cohesin from either *Xenopus* oocyte or human cell extracts is found in the vicinity of cohesin's Smc1/3 heads (Anderson et al., 2002) is clearly consistent with our proposal that Scc1 links the heads together and with the finding that Scc3 binds exclusively to Scc1. The non-SMC material near cohesin's SMC heads in electron micrographs in all likelihood corresponds to Scc1 and Scc3. Our failure to detect co-purification of differently tagged versions of either Scc1, Scc3, Smc1 or Smc3 in soluble and chromatin released cohesin complexes (when expressed in the same yeast cell) suggests the presence of only a single molecule of these four subunits in one cohesin complex. This is in agreement with the findings that the two isoforms of Scc3 in vertebrates, SA1 and SA2, never co-purify in one cohesin complex (Sumara et al., 2000) and that endogenous Scc1 protein cannot be co-immunoprecipitated with a myc-tagged Scc1 from human cell extracts (S. Hauf and J.M. Peters, personal communication). If Scc1 links the heads of Smc1 and Smc3 together, then it appears to link only heads from Smc1 and Smc3 also held together at their hinges.

A new model for sister chromatid cohesion

There have been several proposals for how cohesin might connect sister chromatids. According to one, sisters are joined by a single Smc1/3 hetero-dimer, one of whose heads binds one DNA molecule while the other binds its sister (Toth et al., 1999; Losada and Hirano, 2001; Anderson et al., 2002). According to this model, the gap between sister chromatids is spanned by the hetero-dimer's hinge and coiled regions. The binding of one or both heads is presumably facilitated by cohesin's cleavable Scc1 subunit. Our failure to find more than one molecule of Scc1 associated with the Smc1/3 hetero-dimer means that any bridge of this nature would have to be asymmetric with only one of the two SMC-DNA connections involving Scc1. A variation on this theme would have two different hetero-dimers cooperate in creating the bridge between sisters. One chromatin fibre could be bound by an Smc1 head from one hetero-dimer linked by Scc1 to the Smc3 head from a second one whereas its sister would be bound by the Smc3 head from the first hetero-dimer linked by a second Scc1 molecule to the Smc1 head from the second (Anderson et al., 2002). This model is inconsistent with our finding that both soluble and chromatin released cohesin contain only a single Smc1/3 hetero-dimer and only a single molecule of Scc1 and Scc3. However, we cannot exclude the possibility that cohesin does indeed form multimers when bound to chromatin, but that these higher order complexes are disrupted by nuclease digestion. According to an alternative model, an Smc1/3 hetero-dimer, which is bound to one DNA molecule via both of its heads, is connected with the help of Scc1 to a second hetero-dimer bound to its sister (Losada and Hirano, 2001; Uhlmann et al., 1999). This model predicts that Scc1 would bind either to the Smc1/3's hinge or coiled coils. Our finding that Scc1 has little or no affinity for Smc1/3 hetero-dimers lacking their heads shows that this is not the case.

Our results showing that Scc1 links the two heads of a single Smc1/3 hetero-dimer, thereby creating a huge proteinaceous loop or ring raises yet a third possibility, namely that sister chromatids are held together through their entrapment by a single closed cohesin loop. According to this model, destruction of cohesion by separase is not due to any radical change in the chemistry of cohesin's interaction with DNA but is simply due to breakage of the chromatin fibre's topological enclosure. By supposing that cohesin associates with unreplicated chromatin in a similar if not identical manner, this "embrace" model explains how cohesin can be so tightly associated with chromatin throughout interphase without having a high natural affinity for DNA. It also provides an explanation for the perplexing issue as to how cells ensure that sister DNA molecules but not others are held in cohesin's embrace, why cohesin must be present during DNA replication (Uhlmann and Nasmyth, 1998) and why SMC proteins contain unusually long coiled coil segments. Cohesion between sisters could conceivably be established by replicating through a pre-existing cohesin loop which had previously embraced the unreplicated DNA (Fig. 8B). With a diameter of ~40 nm, cohesin's loop should be large enough to permit passage of a replisome. However, such a feat would be hard to imagine if the diverging forks from a single replicon were held together, as has been suggested in bacteria (Lemon and Grossman, 2000). It is therefore possible that loops which end up embracing sister chromatids are only generated in the replisome's wake.

If correct, the "embrace" model raises important questions as to how cohesin's arms open and shut during its loading onto chromatin. If soluble cohesin is also in a closed form, then it must open before it can embrace a DNA molecule and re-close around it. Several of cohesin's properties may be pertinent to this issue. The first is the potential ATPase activity of its two heads, which could help to drive the embracing process. The second is the finding that cohesin's association with yeast chromatin depends on a second complex containing the Scc2 and Scc4 proteins, which interact only very loosely with cohesin (Ciosk et al., 2000) and might regulate opening and closing. A third concerns the roles of Scc3 and Pds5, which are clearly not required for the formation of closed loops but could easily regulate their opening and/or persistence.

In conclusion, our finding that cohesin has separate Smc1 and Smc3 arms that can be joined by its cleavable Scc1 subunit suggests a novel hypothesis for how sister chromatids are held together after DNA replication. The model's attractions are not the weight of data behind it, which is only modest so far, but rather its explanatory power. It makes a number of testable predictions, not least of which is that cohesion should depend on the integrity of all components of the proposed loop. It is not inconceivable that a protein-DNA inter-catenation principle lies behind the function of other SMC protein complexes.

EXPERIMENTAL PROCEDURES

Thermotoga maritima SMC hinge domain crystal structures

The hinge domain part of SMC (HTMC) from *Thermotoga maritima* (DSMZ No. 3109; TmSMC: TM1182 [SWALL: Q9X0R4]) was amplified by genomic PCR and expressed in E. coli. C41 (Miroux and Walker, 1996) as C-terminal His_6-tag fusions. Two constructs were used in this study: HTMC2 (coding for residues 485-670) and HTMC9 (coding for residues 473-685). Native and Seleno-methionine (SeMet) substituted proteins were produced using NiNTA resin following published procedures (van den Ent et al., 1999). HTMC9 expressing cells were lysed after powdering under liquid nitrogen in a mortar by boiling for 90 seconds to overcome proteolysis problems. All crystals were grown by sitting drop vapour diffusion at 19°C. Monoclinic ($P2_1$), native crystals of HTMC2 were grown using 26% PEG 3000 and 0.1 M CHES pH 9.2 as crystallisation solution. Drops were composed of 2 l protein at 20 mg/ml and 1 l crystallisation solution. SeMet substituted HTMC2 crystals were grown in the same manner as for the native protein but at 10 mg/ml with 30% PEG 3000 and 0.1 M CHES pH 9.2. Orthorhombic crystals of HTMC2 ($P2_12_12_1$) were grown using 15% PEG 2000MME and 0.1 M TRIS pH 6.9 as the crystallisation solution. Drops were composed of 3 l protein at 10 mg/ml and 1 l crystallisation solution. All HTMC2 crystals were frozen in mother liquor complemented with 8-12% glycerol. SeMet HTMC9 protein crystallised in C2 using 0.1M sodium citrate, 0.1M sodium cacodylate and 30% iso-propanol as crystallisation solution. Crystals were frozen in crystallisation solution with 10% isopropanol added.

Diffraction data was collected on beamline 14-1 and 9.5 (SRS, Daresbury, UK) and 14-4 (ESRF, Grenoble, France). Crystal data, dataset- and refinement statistics are summarised in table I and supplemental table S1 at http://www.cell.com/molecular-cell/supplemental/S1097-2765(02)00515-4. Crystals were indexed and integrated using MOSFLM (CCP4) and data were further processed using the CCP4 package (Coll. Comput. Project, N. 4, 1994). An initial 2.5 Å MAD density map of crystal form $P2_1$ was using the program SOLVE (Terwilliger and Berendzen, 1999), which was also used to calculate phases. After solvent flattening, all ordered residues were built into the MAD electron density map using MAIN2001 (Turk, 1992). The structure was refined against all data in dataset $P2_1$ to 2.0 Å resolution using CNS (Brünger et al., 1998). The structure of the SMC hinge domain dimer in the $P2_1$ crystals appeared to be distorted by crystal packing. Dataset $P2_12_12_1$ showed significant twinning when comparing cumulative intensity distributions to those from randomly scattered atoms (TRUNCATE, CCP4). The twinning is a rotation around the c-axis (k, h, -l) facilitated in spacegroup $P2_12_12_1$ by the similarity of the a and b axis. Dataset $P2_12_12_1$ was solved by molecular replacement using the refined $P2_1$ model and CNS, producing only weak solutions. Torsion angle simulated annealing on several solutions picked out the correct one and facilitated a large conformational change in the model that is necessary to convert the $P2_1$ to the $P2_12_12_1$ crystal form. Both crystal forms contained no coiled coil segments – the residues with coiled coil prediction are largely disordered. The longer construct HTMC9 in crystal form C2 was solved by molecular replacement using the undistorted $P2_12_12_1$ model. To verify the initial finding of coiled coil segments in difference densities, and to have an independent indicator of the correctness of the coiled coil arrangement in the model building process, methionine positions and phases were derived from SeMet HTMC9 crystals. Selenium atoms were located using model phases and three strong peaks were detectable on the coiled coil segments. These indicated the positions of M488 and M493 of the N-terminal helix of the coiled coil. The other peak indicated the position of M678 on the C-terminal helix. Phases were calculated from the two HTMC9 SeMet datasets taking the selenium sites as above and were used for refinement and difference electron densities. The C2 datasets have high internal B-factors of about $90Å^2$ (as derived from Wilson plots) that are reflected in the average B-factors of the model. Coordinates and structure factors have been deposited in the Protein Data Bank (table I).

Baculovirus expression vectors

DNA sequences encoding *S. cerevisiae* genes *SMC1*, *SMC3*, *SCC1* or *SCC3* were cloned from genomic library plasmids (Michaelis et al., 1997) into Bac-to-Bac™ (Gibco Life Technologies) pFASTBAC (pFB) baculovirus expression vectors. Epitope tags as described in the individual experiments were introduced at the N- or C-terminus of the respective coding sequence, indicated by the position of the tag name. For detailed descriptions of the constructs, see Supplemental

Expression of yeast proteins in insect cells

Recombinant baculoviruses were obtained by transposition of the expression vectors into DH10BAC cells, bacmid preparation and transfection into Sf9 insect cells (Gibco Life Technologies). Expression of the recombinant proteins was checked by immunoblotting of lysates from transfected cells, and baculoviruses were amplified three times in Sf9 cells to obtain high viral titer stocks in the range of 5×10^8 to 1×10^9 pfu/ml. For protein expression, High Five™ (Invitrogen) insect cells grown at 27°C in Grace's insect media supplemented with 10% fetal calf serum, penicillin, streptomycin and glutamine to near confluency were infected at a multiplicity of infection (MOI) of ~10 for each high titer virus. Cells were harvested 45 hours post-infection and extracts were prepared: cells were washed in ice-cold PBS and broken by hypotonic lysis in a Dounce homogenizer after 10 min swelling in two pellet volumes 50 mM TRIS-HCl pH 8.0, 10 mM KCl containing Complete™ proteinase inhibitor mix EDTA-free (Roche Mol. Biochem.) and PMSF at 0.2 mM. Cytosolic extract was separated from nuclei by 10 min centrifugation at 5,000×g at 4°C. Nuclei were broken after resuspension in two nuclear pellet volumes 50 mM TRIS-HCl pH 8.0, 10 mM KCl, 1.5 mM $MgCl_2$ and proteinase inhibitor mix by increasing the NaCl concentration in three steps to 420 mM final and vortexing after each NaCl addition. Cytosolic and nuclear extracts were cleared by subsequent 30 min high speed centrifugation steps at 40,000×g and 100,000×g at 4°C. Cleared cytosolic and nuclear extracts were then combined.

Gel filtration and glycerol gradient centrifugation

2 ml (resin volume) Ni^{2+}-NTA superflow (QUIAGEN) were pre-equilibrated in T(250/5) buffer (50 mM TRIS-HCl pH 8.0, 10 mM KCl, 1.5 mM $MgCl_2$, first number in brackets refers to NaCl concentration in mM, second number refers to imidazole concentration in mM). Extract prepared from ~4×10^8 infected insect cells (10 T250 flasks) was adjusted to a final concentration of 5 mM imidazole and incubated with the pre-equilibrated Ni^{2+}-NTA resin for 3 to 4 hours shaking at 4°C. The resin was washed sequentially with 10 ml of each T(500,5), T(250,5) twice, T(100,20) and protein was eluted in three steps with 600 l T(100,200) containing 20% glycerol. Eluates were combined.

Half of the eluate from the Ni^{2+}-NTA resin was applied onto a Sephacryl HR300 gel filtration column (Amersham-Pharmacia), using 250 mM NH_4HCO_3, 10 mM TRIS-HCl pH 8.0, 0.2 mM EDTA, 20% glycerol as running buffer. The column was calibrated using standard

proteins (aldolase r_s=4.8 nm, ferrtin r_s=6.1 nm, thyroglobulin r_s=8.5 nm). The Stokes radii for Smc3 and Smc1/3 were calculated following the method of Porath.

15-30% linear glycerol gradients were prepared in 200 mM NH_4HCO_3, 0.2 mM EDTA. 100 l Ni^{2+}-NTA eluate were diluted with 100 l 200 mM NH_4HCO_3, 0.2 mM EDTA and layered on top of the gradient. Gradients were run for 24 h at 38,000 rpm in an SW40Ti rotor (Beckman) and fractionated using an Isco fractionator. For calibration, standard proteins were run in parallel (bovine serum albumine 4.6 S, aldolase 7.3 S, catalase 11.3 S, ferritin 17.6 S, thyroglobulin 19 S) and the S-values of Smc3 and Smc1/3 were calculated by linear regression of the values determined for the standard proteins (R^2=0.99). Presence and purity of Smc3 or Smc1/3 proteins in elution fractions from gel filtration and glycerol gradient centrifugation were determined by silver staining after SDS-PAGE. The native molecular weights of Smc3 and Smc1/3 were calculated using a partial specific volume of 0.725 cm^3/g.

Electron microscopy

3 l of the peak fraction from the Sephacryl column were directly spread on a freshly cleaved 1 cm^2 mica using the sandwiching technique. Micas were dried in vacuum for at least 2 hours before rotary shadowing with 1-2 nm platinum/carbon at an angle of ~8° from an electron beam gun (Bal-Tec, MED 020). Replicas were stabilized with a 5 nm carbon layer, floated onto copper grids and photographed in the electron microscope at 80kV, 25,000× magnification.

Binding assays of baculovirus expressed proteins

Extracts were prepared from ~4×10^7 insect cells 45 hours after co-infection with recombinant viruses as indicated. 200 l cleared extract were diluted with 800 l T(250,0) plus 0.2 mM PMSF. For binding assays on Ni^{2+}-NTA, diluted extracts were adjusted to 5 mM imidazole and incubated with 100 l pre-equilibrated Ni^{2+}-NTA superflow resin (QUIAGEN) for 3 hours at 4°C. The Ni^{2+}-NTA resin was washed with 1 ml of each T(500,5), T(250,5) twice, T(100,20) and bound protein was eluated with 100 μl T(250,150). For co-immunoprecipitations, 5 μl 16B12 monoclonal antibody (BAbCO) were added to diluted extracts and allowed to bind to the HA-epitope for 1.5 hours shaking at 4°C before addition of 50 μl pre-equilibrated proteinG sepharose (Amersham-Pharmacia). After shaking at 4°C for another 2.5 hours, beads were washed 3 times in T(250,0) and bound protein was eluted by boiling in 100 l SDS-loading buffer. Proteins were separated by SDS-PAGE and detected by immunoblotting, using

a polyclonal antibody raised against the N-terminus of Smc1 (a gift from C. Frei and S. Gasser, Lausanne) or monoclonal antibodies against the His$_6$ (Penta·His, Sigma), HA (16B12, BAbCO), FLAG (M2, Sigma) or myc-epitopes (9E10).

Binding assays on proteins isolated from yeast

All strains used were derivatives of W303 and carried a deletion of the PEP4 protease gene to reduce protein degradation during extract preparation and immunoprecipitations. Strains expressing cohesin subunits tagged C-terminally with multiple copies of either the HA- or myc-epitope from their original genomic loci were described previously and have been shown to be functional in vivo (Michaelis et al., 1997; Toth et al., 1999). These strains were crossed to obtain diploid strains as indicated in the figures. Extracts from asynchronous yeast cultures were prepared following the protocol by Liang and Stillman (Liang and Stillman, 1997), with the exception that zymolyase T100 at 40 g/ml was used for spheroblasting and Complete™ proteinase inhibitor mix (Roche Mol. Biochem.) and 0.2 mM PMSF replaced the proteinase inhibitors in the EB buffer. Chromatin pellets were separated from the soluble fraction and cohesin complexes were released from chromatin pellets by micrococcal nuclease treatment as published (Ciosk et al., 2000). Co-immunoprecipitations were carried out as described for baculovirus expressed proteins, with the exception that soluble and chromatin released fractions were pre-cleared with proteinG sepharose before the addition of antibody.

BIAcore measurements

All experiments were carried out at a flow rate of 5 l/min using HBS plus 0.005% Surfactant P20 as running buffer. Rabbit anti-mouse Fc-γ antibody (BIAcore) was immobilized to a CM5 sensor chip surface at a concentration of 30 g/ml in 10 mM Na-acetate pH 5.0 using standard EDC/NHS crosslinking procedure. 12CA5 (anti-HA) was loaded as secondary antibody (followed by 10 1 1M NaCl wash) to bind HASmc3 or HASmc3hinge from cleared insect cell extracts. Cleared extract from insect cells expressing Smc1 were floated over the loaded sensor and association- and dissociation-phases were recorded for 10 and 30 min, respectively. The sensor chip was regenerated with 30 mM HCl and 1M NaCl and the experiment was repeated with a different dilution of Smc1 extract. The concentration of Smc1 in the extract was estimated by quantitative immunoblotting using purified Smc1 as standard, and extracts were diluted with uninfected insect cell extracts to obtain Smc1 concentrations from 20 to 200 nM. For all dilutions, Smc1 binding on lanes loaded only with

secondary antibody was recorded and substracted from the curves to account for unspecific binding.

REFERENCES

Anderson, D. E., Losada, A., Erickson, H. P., and Hirano, T. (2002). Condensin and cohesin display different arm conformations with characteristic hinge angles, J Cell Biol *156*, 419-24.

Brunger, A. T., Adams, P. D., Clore, G. M., DeLano, W. L., Gros, P., Grosse-Kunstleve, R. W., Jiang, J. S., Kuszewski, J., Nilges, M., Pannu, N. S.*, et al.* (1998). Crystallography & NMR system: A new software suite for macromolecular structure determination, Acta Crystallogr D Biol Crystallogr *54*, 905-21.

Buonomo, S. B., Clyne, R. K., Fuchs, J., Loidl, J., Uhlmann, F., and Nasmyth, K. (2000). Disjunction of homologous chromosomes in meiosis I depends on proteolytic cleavage of the meiotic cohesin Rec8 by separin, Cell *103*, 387-398.

Ciosk, R., Shirayama, M., Shevchenko, A., Tanaka, T., Toth, A., Shevchenko, A., and Nasmyth, K. (2000). Cohesin's binding to chromosomes depends on a separate complex consisting of Scc2 and Scc4 proteins, Mol Cell *5*, 243-254.

Coll. Comput. Project, N. 4 (1994). The CCP4 Suite: Programs for Protein Crystallography, Acta Crystallographica D *50*, 760-763.

de Jager, M., van Noort, J., van Gent, D. C., Dekker, C., Kanaar, R., and Wyman, C. (2001). Human Rad50/Mre11 is a flexible complex that can tether DNA ends, Mol Cell 8, 1129-35.

Hauf, S., Waizenegger, I., and Peters, J. M. (2001). Cohesin cleavage by separase required for anaphase and cytokinesis in human cells, Science 293, 1320-3.

Hirano, T., Kobayashi, R., and Hirano, M. (1997). Condensins, chromosome condensation protein complexes containing XCAP-C, XCAP-E, and a Xenopus homolog of the Drosophila Barren protein, Cell 89, 511-521.

Hirano, M., Anderson, D. E., Erickson, H. P., and Hirano, T. (2001). Bimodal activation of SMC ATPase by intra- and inter-molecular interactions, EMBO J 20, 3238-50.

Holm, L. and Sander, C. (1995). Dali: a network tool for protein structure comparison, Trends Biochem Sci 20, 478-80

Hopfner, K. P., Karcher, A., Shin, D. S., Craig, L., Arthur, L. M., Carney, J. P., and Tainer, J. A. (2000). Structural biology of Rad50 ATPase: ATP-driven conformational control in DNA double strand break repair and the ABC-ATPase superfamily, Cell 101, 789-800.

Kraulis, P. J. (1991). MOLSCRIPT: a program to produce both detailed and schematic plots of protein structures, Journal of Applied Crystallography 24, 946-50.

Lemon, K. P., and Grossman, A. D. (2000). Movement of replicating DNA through a stationary replisome, Mol Cell 6, 1321-30.

Liang, C., and Stillman, B. (1997). Persistent initiation of DNA replication and chromatin-bound MCM proteins during the cell cycle in cdc6 mutants, Genes Dev 11, 3375-86.

Losada, A., Hirano, M., and Hirano, T. (1998). Identification of Xenopus SMC protein complexes required for sister chromatid cohesion., Genes Dev 12, 1986-1997.

Losada, A., and Hirano, T. (2001). Intermolecular DNA interactions stimulated by the cohesin complex in vitro. Implications for sister chromatid cohesion, Curr Biol 11, 268-272.

Löwe, J., Cordell, S. C., and van den Ent, F. (2001). Crystal structure of the SMC head domain: an ABC ATPase with 900 residues antiparallel coiled-coil inserted, J Mol Biol 306, 25-35.

Melby, T. E., Ciampaglio, C. N., Briscoe, G., and Erickson, H. P. (1998). The symmetrical structure of structural maintainance of chromosomes (SMC) and MukB proteins: Long, antiparallel coiled coils, folded at a flexible hinge, J Cell Biol 142, 1595-1604.

Michaelis, C., Ciosk, R., and Nasmyth, K. (1997). Cohesins: Chromosomal proteins that prevent premature separation of sister chromatids., Cell 91, 35-45.

Miroux, B., and Walker, J. E. (1996). Over-production of proteins in Escherichia coli: mutant hosts that allow synthesis of some membrane proteins and globular proteins at high levels, J Mol Biol 260, 289-98.

Nasmyth, K. (2001). DISSEMINATING THE GENOME: Joining, Resolving, and Separating Sister Chromatids During Mitosis and Meiosis, Annu Rev Genet 35, 673-745.

Neuwald, A. F., and Hirano, T. (2000). HEAT Repeats Associated with Condensins, Cohesins, and Other Complexes Involved in Chromosome-Related Functions, Genome Res 10, 1445-1452.

Panizza, S., Tanaka, T., Hochwagen, A., Eisenhaber, F., and Nasmyth, K. (2000). Pds5 cooperates with cohesin in maintaining sister chromatid cohesion, Curr Biol 10, 1557-1564.

Pasierbek, P., Jantsch, M., Melcher, M., Schleiffer, A., Schweizer, D., and Loidl, J. (2001). A Caenorhabditis elegans cohesion protein with functions in meiotic chromosome pairing and disjunction, Genes Dev 15, 1349-60.

Rao, H., Uhlmann, F., Nasmyth, K., and Varshavsky, A. (2001). Degradation of a cohesin subunit by the N-end pathway is essential for chromosome stability, Nature 410, 955-959.

Siegel, L. M., and Monty, K. J. (1966). Determination of molecular weights and frictional ratios of proteins in impure systems by use of gel filtration and density gradient centrifugation. Application to crude preparations of sulfite and hydroxylamine reductases, Biochim Biophys Acta 112, 346-62.

Sonoda, E., Matsusaka, T., Morrison, C., Vagnarelli, P., Hoshi, O., Ushiki, T., Nojima, K., Fukagawa, T., Waizenegger, I. C., Peters, J.

M., *et al.* (2001). Scc1/Rad21/Mcd1 is required for sister chromatid cohesion and kinetochore function in vertebrate cells, Dev Cell *1*, 759-70.

Soppa, J. (2001). Prokaryotic structural maintenance of chromosomes (SMC) proteins: distribution, phylogeny, and comparison with MukBs and additional prokaryotic and eukaryotic coiled-coil proteins, Gene *278*, 253-64.

Sumara, I., Vorlaufer, E., Gieffers, C., Peters, B. H., and Peters, J.-M. (2000). Characterization of vertebrate cohesin complexes and their regulation in prophase, J Cell Biol *151*, 749-762.

Terwilliger, T. C. and Berendzen, J. (1999). Automated MAD and MIR structure solution, Acta Crystallographica Section D-Biological Crystallography *55*, 849-861.

Toth, A., Ciosk, R., Uhlmann, F., Galova, M., Schleifer, A., and Nasmyth, K. (1999). Yeast Cohesin complex requires a conserved protein, Eco1p (Ctf7), to establish cohesion between sister chromatids during DNA replication, Genes Dev *13*, 320-333.

Turk, D. (1992), Weiterentwicklung eines Programms für Molekülgrafik und Elektrondichte-Manipulation und seine Anwendung auf verschiedene Protein-Strukturaufklärungen, Ph. D. Thesis, Technische Universität München

Uhlmann, F., and Nasmyth, K. (1998). Cohesion between sister chromatids must be established during DNA replication, Current Biology *8*, 1095-1101.

Uhlmann, F., Lottspeich, F., and Nasmyth, K. (1999). Sister chromatid separation at anaphase onset is promoted by cleavage of the cohesin subunit Scc1p, Nature *400*, 37-42.

Uhlmann, F., Wernic, D., Poupart, M. A., Koonin, E., and Nasmyth, K. (2000). Cleavage of cohesin by the CD clan protease separin triggers anaphase in yeast, Cell *103*, 375-386.

van den Ent, F., Lockhart, A., Kendrick-Jones, J., and Lowe, J. (1999). Crystal structure of the N-terminal domain of MukB: a protein involved in chromosome partitioning, Structure Fold Des *7*, 1181-7.

Waizenegger, I., Hauf, S., Meinke, A., and Peters, J. M. (2000). Two distinct pathways remove mammalian cohesin from chromosome arms in prophase and from centromeres in anaphase, Cell *103*, 399-410.

SUPPLEMENTAL MATERIAL

Baculovirus expression vectors

To clone pFB Smc1 hinge, the part of the *SMC1* gene in pFB Smc1 encoding the hinge domain (aa residues 500 to 696) was removed by *Cla*I restriction digest. The DNA sequence coding for Smc3 residues 512 to 670 was then inserted into the *Cla*I-site to obtain Smc1hinge3. By replacing the *Aat*II/*Bsg*I restriction fragment of the *SMC3* gene in pFB His$_6$Smc3 with a PCR generated DNA sequence encoding the hinge domain of Smc1 and part of the C-terminal coiled-coil domain of Smc3, aa residues 512 to 676 of Smc3 were swapped to aa residues 506 to 706 of Smc1, giving pFB His$_6$Smc3hinge1. Parts of the *SMC3* gene encoding the individual globular domains of Smc3 were cloned by PCR (aa 1 to 170, N-terminus, aa 484 to 684, hinge domain, aa 1046 to 1230, C-terminus). To yield pFB HA$_3$Smc1 head and pFB Smc3 headHis$_6$, we cloned the part of the *SMC1* gene encoding aa residues 175 to 1063 and the part of the *SMC3* gene encoding aa residues 172 to 1042 by PCR. We then inserted the coding sequence of the human fibronectin cell adhesion domain, FN7-10 (Melby et al., 1998), at the N- and C-terminus of pFB Smc3 headHis$_6$ to gain pFB FNSmc3FNHis$_6$. To express the isolated Smc3 head domain, we amplified sequences encoding the N-terminal (aa 1 to 170) and C-terminal (aa 1041 to 1230) globular domains of Smc3 and connected them by a sequence encoding a 14 aa linker described previously (Löwe et al., 2001). Addition of an N-terminal HA$_3$ epitope tag by PCR resulted in pFB HA$_3$Smc3hdI. N-terminal (aa 1 to 180) and C-terminal (aa 269 to 566) Scc1 fragments as well as full length Scc1 were cloned by PCR, adding a sequence tag encoding six histidine residues with the primer. The FLAG tagged version of Scc1 fused to a chitin binding domain was described previously (Uhlmann et al., 2000).

Supplemental Table I: crystallographic data

P2$_1$:   HTMC2, *T. maritima* SMC hinge domain, residues 485-670

a=54.7 Å, b=57.9 Å, c=62.5 Å, β=112.4°, two molecules/ASU

P2$_1$2$_1$2$_1$:   HTMC2

a=58.9 Å, b=62.2 Å, c=225.1 Å, twinning fraction 0.158, four molecules/ASU

C2   HTMC9, *T. maritima* SMC hinge domain, residues 473-685

a=136.7 Å, b=115.9 Å, 69.4 Å, β=93.4°, four molecules/ASU

Dataset	λ[Å]	SG	resol.[Å]	I/σI[1]	Rm[2]	multipl.[3]	compl.[%][4]
P2$_1$	0.9393	P2$_1$	2.0	12.2(4.3)	0.072	2.2	95.0
P2$_1$PK1	0.9784	P2$_1$	2.5	25.4(10.3)	0.037	5.1	98.8
P2$_1$PK2	0.9784	P2$_1$	2.5	27.1(10.4)	0.033	4.8	96.1
P2$_1$IN1	0.9793	P2$_1$	2.5	23.9(9.1)	0.040	5.1	98.9
P2$_1$IN2	0.9793	P2$_1$	2.5	31.2(12.0)	0.035	6.4	96.1
P2$_1$RE1	0.9500	P2$_1$	2.5	22.8(8.6)	0.044	5.1	98.8
P2$_1$RE2	0.9500	P2$_1$	2.5	29.3(8.7)	0.037	6.2	96.1
P2$_1$2$_1$2$_1$	0.9393	P2$_1$2$_1$2$_1$	3.0	10.6(3.1)	0.093	2.8	92.7
C2PK1	0.9793	C2	3.0	16.3(2.9)	0.075	5.1	95.1
C2PK2	0.9793	C2	3.2	16.2(4.4)	0.059	3.9	95.3

[1]signal to noise ratio of intensities, highest resolution bin in brackets. [2]R$_m$: $\Sigma_h\Sigma_i|I(h,i)-I(h)| / \Sigma_h\Sigma_i I(h,i)$ where I(h,i) are symmetry related intensities and I(h) is the mean intensity of the reflection with unique index h. [3]Multiplicity for unique reflections, for MAD datasets I(+) and I(-) are kept separate. [4]Completeness of unique reflections, merged Friedel pairs. Correlation coefficients of anomalous differences at different wavelengths for the MAD experiment in P2$_1$: PEAK1 versus INFL1: 0.36, PEAK1 versus HREM1: 0.40, INFL1 versus HREM1: 0.28.
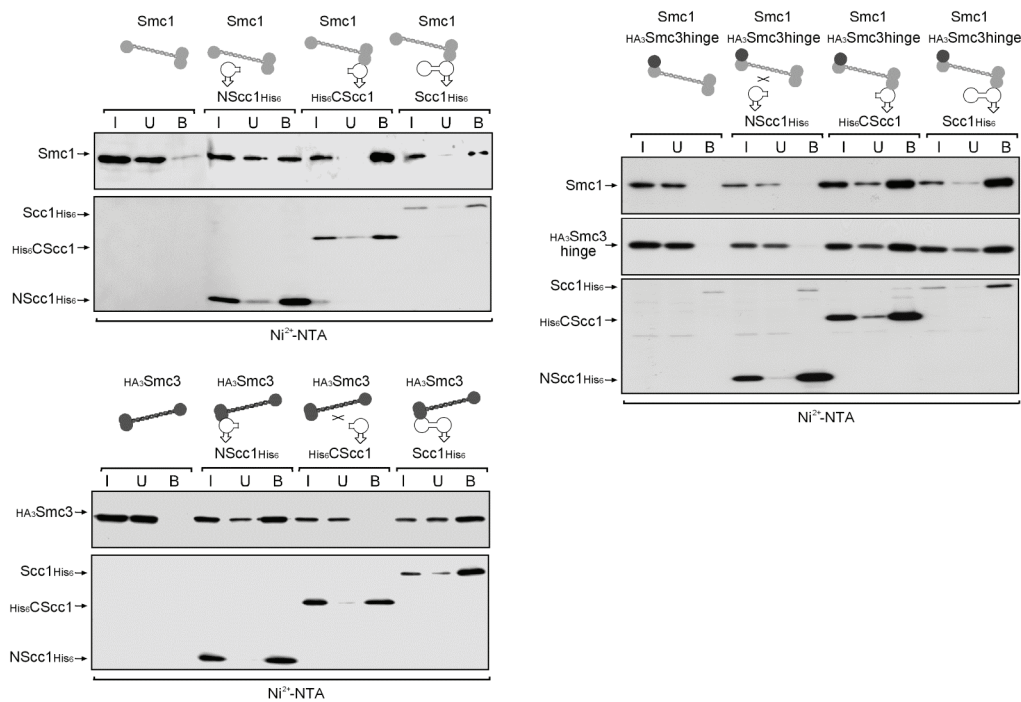
Supplemental Figure S1 Smc1 preferentially binds the C-terminal and Smc3 only binds the N-terminal separase cleavage fragment of Scc1. Smc1 or HA$_3$Smc3 were co-expressed with His$_6$-tagged N- and C-terminal Scc1 fragments or full length Scc1 and run over Ni^{2+}-NTA. Co-purification of Smc1 or HA$_3$Smc3 with His$_6$Scc1 (fragments) in input (I), unbound (U) or imidazole eluate (bound, B) fractions were probed with specific antibodies. Simultaneous co-expression of an HA3-tagged version of the Smc3 hinge domain with Smc1 eliminated the weak binding of Smc1 to the N-terminal Scc1 fragment (right panel).